

Thermal Analysis on Voltage Responses of High- T_c Superconducting Thin-Films Exposed to a Pulse Laser Beam

Jae-Mo Koo* and Seungho Park**

(Received April 10, 1997)

One-dimensional radiation/conduction heat transfer model is employed to investigate thermal responses of HTSC thin-film detectors exposed to a pulse laser beam. The theoretical model includes local radiation absorption in the HTSC film based on the electromagnetic theory, thermal contact resistances at the interface between film and substrate, and nonuniform initial condition for the film/substrate temperature incurred by the Joule heating due to the bias current and inherent electrical resistance even before the radiation exposure. Using the steady-state conduction equation, the experimental resistance-temperature curve is corrected based on the real film temperatures instead of the substrate temperatures. The error involved in the estimation of the voltage jump based on the model without initial Joule heating could be significant near the transition temperature. Still there is a big discrepancy between the theoretical and experimental results, though the nonuniform initial condition model reduces the gap.

Key Words: Voltage Response, High- T_c Superconductor, Radiation Detector, Nonuniform Initial Condition

Nomenclature

Bi	: Biot number		Joule heating (W/m^3)
C	: Specific heat of phonon (J/kgK)	q''_{rad}	: Volumetric heat generation by radiation absorption (W/m^3)
c	: Specific heat (J/kgK) or speed of light (m/s)	r	: Electrical resistance (Ω)
d	: Thickness (m)	r_d	: Thickness ratio of interfacial-layer to the film
E	: Electrical field (V/m)	r_h	: Conductivity ratio of interfacial-layer to the film
h_b	: Thermal contact heat transfer rate (W/m^2K)	R_b	: Thermal contact resistance (m^2K/W)
I	: Bias current (A)	$S(x)$: Normalized source function
k	: Thermal conductivity (W/mK)	t	: Time (s)
l	: Mean free path of phonon (m)	t_f	: Fall time (s)
n	: Real part of refractive index	t_l	: Time lag (s)
N	: Complex refractive index	t_p	: Pulse length, full width at half maximum (s)
q''_b	: Heat flux at the film/substrate interface (W/m^2)	T	: Temperature (K)
q''_i	: Incident radiative power (W/m^2)	T_0	: Initial substrate temperature (K)
q''_{rad}	: Energy flux absorbed in the film (W/m^2)	T_c	: Critical temperature of high T_c superconductor (K)
$q''_{f, resist}$: Volumetric heat generation in the film by	v	: Speed of sound (m/s)
		V	: Voltage (V)
		\forall	: Volume of film (m^3)
		ΔV_{max}	: Maximum voltage response (V)

* Graduate School, Hongik University, Seoul 121-791, Korea

** Department of Mechanical Engineering, Hongik University, Seoul 121-791, Korea

x : Distance from the front surface of film
(m)

Greek Letters

Δ : Difference
 χ : Imaginary part of refractive index
 λ : Wavelength of incident radiation (m)
 ρ : Density (kg/m^3)
 τ_h : Relaxation time for heat flow (s)

Subscripts

avg : Averaged value
b : Interface between film and substrate
f : Film
i : Incident radiation
I : Interfacial layer
max : Maximum value
rad : Thermal radiation
resis : Joule heating
s : Substrate

1. Introduction

Since the discovery of high- T_c superconductor (HTSC), intense investigations have been focused on the application of the superconducting thin films due to their superior superconducting properties compared with those of bulk material. HTSC thin film applications include SQUID, tunnel junction, a fast nonlinear switch for noise discrimination in digital circuits, etc. Such high- T_c superconducting devices have attracted a great deal of attention as broadband optical (infrared and visible) detectors (Frenkel et al., 1990). One of the first major applications of thinfilm HTSC is a superconducting detector which is called a bolometer and is suitable for lowtemperature environmental or space applications (Brasunas et al., 1989; Flik et al., 1990).

A bolometer is a device that senses incident electromagnetic radiation by absorbing the radiant energy, bringing about temperature increase, and thus changing the electrical resistance, and finally resulting in the voltage jump (Flik et al., 1990). So far bolometers have been made mainly

from the semiconductor and low-temperature superconductors (LTSC). LTSC bolometers have a capability of detecting the radiation from X-ray to microwave of spectrum. However, due to the complexity of the devices, these are rarely used in practice (Frenkel et al., 1990). Richards et al. (1989) indicated that thin-film HTSC bolometers were more sensitive than conventional 77 K bolometers in the detection of infrared radiation and concluded that they were promising.

Voltage response of a HTSC bolometer to incident radiation consists of thermal (bolometric, equilibrium) and nonequilibrium (nonbolometric, nonthermal) responses (Frenkel et al., 1990; Zeldov et al., 1989). Thermal response is the voltage change due to the temperature rise by absorbing incident radiation in the film, while nonbolometric response has been understood generally as a result from the direct interaction between photons and superconducting electrons (Cooper pairs) in the film (Frenkel et al., 1990). The thermal response is strong at temperatures in the transition region from the superconducting state to the normal one and is the most sensitive mechanism that has been carefully documented and understood. The nonbolometric response, which is faster, is dominant at temperatures below the transition region, showing weak temperature dependence and a linear dependence on the bias current. Here, only the bolometric responses are analyzed, because nonbolometric phenomena are based on unclear nonthermal mechanisms and are known to be dominant at temperatures well below the critical temperature, T_c .

Several prototypes have been already experimented to understand the factors affecting bolometer signal (Carr et al., 1990; Frenkel et al., 1990; Zeldov et al., 1989; Zorin et al., 1995) and theoretical models have been developed to depict their behavior. Kumar and Joshi (1990) presented a parametric study of examining the effects of incoming radiation flux and bias current on the sensitivity and response of a bolometer. Flik et al. (1990) presented a rigorous thermal analysis of superconducting bolometers.

Fushinobu et al., (1994) performed a thermal

analysis of bolometer exposed to a periodic pulse laser beam, deriving a periodic steady-state heat conduction equation. Chen et al. (1995) introduced a skin-depth model for the prediction of radiation absorption and the interfacial-layer model for thermal contact resistance at the interface between the film and the substrate. Very wide, however, is the gap between the experimental data and theoretical calculations which are reasonable only qualitatively. Therefore, the objective of this study is to examine the important governing factors, to describe the phenomena more clearly, and to narrow the gap.

In this study, heat transfer phenomena in a bolometer exposed to an optical pulse have been described as a conjugate radiation/conduction process including important factors such as temperature-dependent thermophysical properties, absorption of incident radiation based on the electromagnetic theory, thermal contact resistance at the interface between the film and the substrate, Joule heating, and nonuniform initial conditions due to the bias current and electric resistance which has never been recognized in previous studies. In addition, using the steady-state conduction equation, the experimental resistance-temperature curve is corrected based on the real film temperatures instead of the substrate or cold finger temperatures.

2. Thermal Analysis

Schematic diagram of a HTSC thin-film radiation detector is shown in Fig. 1, where q_i'' is incident radiation, I , a bias current, and d_f and d_s , thicknesses of the film and the substrate, respectively. Heat transfer in the HTSC bolometer exposed to incident radiation is modeled as a one-dimensional conjugate radiation/conduction process.

2.1 Governing equations and boundary conditions

For the HTSC film/substrate system, one-dimensional Fourier conduction equations with variable properties are given by

for film

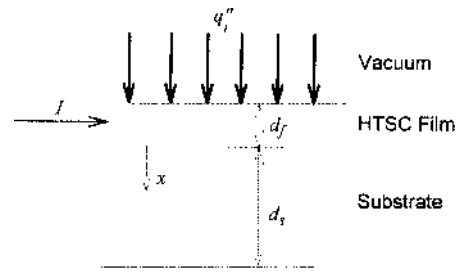


Fig. 1 Schematic diagram of a HTSC thin-film radiation detector.

$$\rho_f c_f \frac{\partial T_f}{\partial t} = \frac{\partial}{\partial x} \left(k_f \frac{\partial T_f}{\partial x} \right) + q_{f,rad}''' + q_{f,resis}''' \quad (1)$$

for substrate

$$\rho_s c_s \frac{\partial T_s}{\partial t} = \frac{\partial}{\partial x} \left(k_s \frac{\partial T_s}{\partial x} \right) + q_{s,rad}''' \quad (2)$$

where T is temperature, ρ , density, c , specific heat, k , thermal conductivity, and q''' , volumetric heat source, respectively. Subscripts *rad*, *resis*, *f* and *s* denote radiation absorption, Joule heating, film, and substrate, respectively. Boundary conditions for the governing equations are given by

$$\begin{aligned} \frac{\partial T_f}{\partial x} \Big|_{x=0} &= 0, \\ -k_f \frac{\partial T_f}{\partial x} \Big|_{x=d_f} &= -k_s \frac{\partial T_s}{\partial x} \Big|_{x=d_f} = q_b'', \\ T_s(d_f + d_s, t) &= T_0 \end{aligned} \quad (3)$$

where q_b'' is heat flux at the film/substrate interface which could be obtained from the thermal contact resistance model and T_0 , initial substrate temperature.

At cryogenic temperatures thermal contact resistance between two dielectrics or between a metal and a dielectric can be several orders of magnitude higher than that at room temperature (Phelan et al., 1990). For temperatures lower than about 30K this can be well explained by the acoustic mismatch theory (AMT) (Little, 1959). For temperatures above about 50K, thermal contact resistance can be modeled by interfacial-layer model (ILM) based on the experimental observations (Marshall et al., 1992).

The AMT assumes the steady-state acoustic mismatch between the solid-solid interface and tells that thermal contact resistance is propor-

tional to the inverse of the third power of the temperature and therefore increases significantly with decreasing temperature. The AMT agrees with measurements only for temperatures below about 30K. At temperatures higher than about 30K, the AMT predicts the thermal contact resistance R_b much lower than measured values at solid-solid interfaces (Swartz and Pohl, 1989).

The ILM assumes there is a layer of variable thickness (about 1-10 % of the total film thickness) inside of the superconducting film and the diffusivity of the layer is significantly lower (about 10-100 times) than that of bulk material (Marshall et al., 1992). The Biot number Bi defined as $h_b d_f / k_f$, in the ILM is r_k / r_d , where r_k is the conductivity ratio and r_d is the thickness ratio of the interfacial imaginary layer to the film. Here, h_b is the contact conductance and is equal to $1/R_b$. The temperature range of concern in this study is between 50 K and 80 K, where the ILM will give more accurate predictions for R_b . Therefore, the interfacial-layer model is mainly employed in the study.

2.2 Nonuniform initial temperature distribution

Initial conditions used by previous investigators (Flik et al., 1990; Chen et al., 1995) are as follows ;

$$T_f(x, 0), \quad T_s(x, 0) = T_0 \quad (4)$$

which assumes that the temperatures of the film and the substrate are initially uniform and maintained at the same temperature before the radiation incidence.

In its vortex state, HTSC film has a finite electrical resistance and thus Joule heating due to the resistance and the bias current occurs in the film. Since the heat generated in the film causes a temperature rise in the film and is supposed to leave the bolometer through the substrate, the temperature fields of the film/substrate must be nonuniform even before the radiation incidence, which will be included in this study. The nonuniform initial conditions can be obtained by solving the steady-state conduction equations given as

$$0 = \frac{\partial}{\partial x} \left(k_f \frac{\partial T_f}{\partial x} \right) + q_f''', \text{resis} \quad (0 \leq x \leq d_f) \quad (5)$$

$$0 = \frac{\partial}{\partial x} \left(k_s \frac{\partial T_s}{\partial x} \right) \quad (d_f \leq x \leq d_f + d_s) \quad (6)$$

with boundary conditions, Eq. (3).

This preheating effect due to the bias current, also, should be included in the accurate calibration of the electrical resistance of the HTSC film. In most experiments, the resistance of the film is read at the temperature of the substrate ($x = d_f + d_s$) or the cold finger, not at the real film temperature. If in its superconducting state, this makes no difference due to zero resistance. If in the vortex or normal state, there might exist a temperature difference between the film and the temperature measuring points and thus the reference temperature for the resistance must be given to the film temperature.

2.3 Radiation absorption and Joule heating

The portion of the incident radiant energy absorbed in the film/substrate is strongly dependent on the wavelength of incident radiation and the refractive indices and thicknesses of the film and the substrate. The local distribution of radiation absorption in the film and substrate can be calculated using the electromagnetic theory (Tuntomo et al., 1991) by

$$q_f''', \text{rad} = \frac{4\pi n_f k_f}{\lambda} S_f(x) q_i'',$$

$$q_s''', \text{rad} = \frac{4\pi n_s k_s}{\lambda} S_s(x) q_i'' \quad (7)$$

where q_i'' is incident radiation flux, λ , wavelength of the radiation, n and k , real and imaginary parts of refractive index of the material, respectively. Normalized source functions $S(x)$ are given by

$$S_f(x) = \frac{|E_f|^2}{|E_i|^2}, \quad S_s(x) = \frac{|E_s|^2}{|E_i|^2} \quad (8)$$

where E_i is the incident electric field strength and E , electric field strength in the film or substrate. The normalized source functions are obtained using plane-wave solutions of the electromagnetic theory (Koo, 1996).

At its vortex state HTSC film exhibits a finite electrical resistance. As the temperature of the

film changes, voltage change occurs due to the change of film resistance and the imposition of the bias current. The voltage for a given temperature distribution is given as (Kumar and Joshi, 1990)

$$\Psi = Id_f \left[\int_0^{d_f} \frac{dx}{r \left[I, \frac{T_f(x)}{T_f(x)} \right]} \right]^{-1} \quad (9)$$

where r is the electrical resistance of the HTSC film. Local Joule heat generation per unit volume is given as (Chen et al., 1995)

$$q_{f, \text{resis}}'' = \frac{(Id_f)^2}{r \left[I, \frac{T_f(x)}{T_f(x)} \right]} \left[\int_0^{d_f} \frac{dx}{r \left[I, \frac{T_f(x)}{T_f(x)} \right]} \right]^{-2} \Psi^{-1} \quad (10)$$

where Ψ is the volume of the film.

2.4 Configuration of HTSC bolometer

To compare the current results with those of other previous investigations, the configuration of the bolometer is chosen to be the same as those of the experimental work (Frenkel et al., 1990) and theoretical studies (Flik et al., 1990; Chen et al., 1995). The HTSC thin film bolometer consists of YBCO ($\text{YBa}_2\text{Cu}_3\text{O}_7$) superconducting bridge and MgO substrate. The rectangular superconducting YBCO film is 200 μm long, 50 μm wide, and 40 nm thick. The MgO substrate is 1 mm thick. Refractive indices for the film and the substrate are assumed to be constant as $N_f = 1.65 + 0.78i$ and $N_s = 1.73 + (1.45 \times 10^{-6})i$. Incident laser pulses are modeled as gaussian-shaped pulses and of two durations: full-width-at-half-maximum, t_p , of 200 ns and 150 ps. The wavelength of incident radiation is 1.06 μm . The incident radiant flux for the 200 ns long pulse can be represented by (Flik et al., 1990)

$$q_i'' = (3.81 \times 10^7) \exp \left[-\frac{(t/t_p - 1)^2}{0.36067} \right] (\text{W/m}^2) \quad (11)$$

and for the 150 ps long pulse by

$$q_i'' = (6.38 \times 10^9) \exp \left[-\frac{(t/t_p - 2)^2}{0.36067} \right] (\text{W/m}^2) \quad (12)$$

Temperature functions for k_f (Hagen et al., 1989), k_s (Slack, 1962), c_f (Ferreira et al., 1988; van Miltenburg et al., 1987) and c_s (Touloukian and Buyco, 1970) used in the following numerical

analysis for the Fourier equations.

for YBCO film

$$\begin{aligned} k_f &= 0.814 T^{0.229} \text{ W/mK} & (4 \leq T \leq 100\text{K}) \\ c_f &= 7.964 \times 10^{-3} (T-4)^{2.480} + 0.10 \text{ J/kgK} \\ & & (4 \leq T \leq 45\text{K}) \\ &= 2.653 (T-45)^{0.970} + 79.69 \text{ J/kgK} \\ & & (45 \leq T \leq 100\text{K}) \\ \rho_f &= 6350 \text{ kg/m}^3 & (13) \end{aligned}$$

for MgO substrate

$$\begin{aligned} k_s &= 24.709 (T-4)^{1.458} + 37 \text{ W/mK} \\ & & (4 \leq T \leq 30\text{K}) \\ &= 2893.84 - 657.93 (T-30)^{0.337} \text{ W/mK} \\ & & (30 \leq T \leq 100\text{K}) \\ c_s &= 0.033 + 5.083 \times 10^{-4} (T-4)^{2.813} \text{ J/kgK} \\ \rho_s &= 3580 \text{ kg/m}^3 & (14) \end{aligned}$$

where k represents the transverse conductivity, not the in-plane one.

3. Results and Discussion

For a short time-scale considered in the present analysis, the validity of the Fourier diffusion equation can be questionable. The Fourier equations could be applicable in the analysis of heat transfer if the relaxation time for heat flow, τ_h , is much smaller than the time of interest. A rough approximation for τ_h is given as (Flik et al., 1990)

$$\tau_h \approx l/v \quad (15)$$

where l is the mean free path (MFP) and v , average speed of the heat carriers. Since phonons are the primary heat carriers in most high- T_c superconductors, v is the speed of sound. By kinetic theory the phonon MFP l can be estimated from (Kittel, 1986)

$$k = \frac{1}{3} \rho C v l \quad (16)$$

where k is the thermal conductivity, ρ , density, and C , heat capacity of phonon, respectively. In this analysis the time of interest is the duration of the shortest pulse, t_p (in this study, $t_p = 150$ ps). If t_p is much larger than τ_h , the Fourier equation is applicable in thermal analysis of the bolometer. Otherwise, the Fourier equation involves signifi-

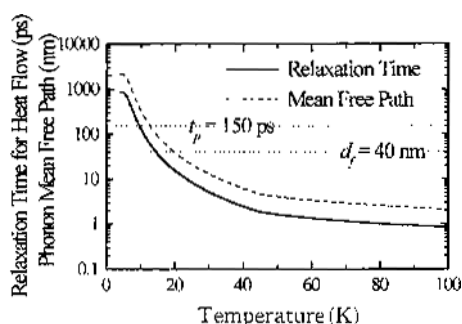


Fig. 2 Relaxation times (τ_h) and phonon mean free paths (l) with respect to film temperatures.

cant errors.

Figure 2 compares the relaxation times, τ_h , of the YBCO film and the characteristic pulse time, t_p . Since τ_h is longer than t_p at temperatures below 10 K, the Fourier equation does not hold for this low temperature range. In the temperature range of concern, above 40 K, τ_h has a value of order 1 ps and thus the application of the Fourier equation is justified.

In addition the phonon MFP, l , and the thickness of film, d_f are compared in this figure. If the heat carrier MFP is of the same order of magnitude as or longer than the film thickness, thermal conductivity will be decreased from its bulk value. Near and below 20K, the MFP has the values of the same order of magnitude as or less than d_f and thus the size effect should be considered. For the situation considered here, the size effecty is not significant since the MFP is much smaller than the film thickness for the temperature range of interest. As the temperature decreases, however, size effects become more significant and should be considered in the analysis.

Figure 3 compares the original resistance-temperature (r - T) curve (Frenkel et al., 1990) and the corrected one from the model discussed in Sec. 2.2 where the bias current, I , is set at 5 mA. The experimental r - T curve is read at the substrate temperature and the corrected one is based on the real HTSC film temperatures which are calculated using the steady-state Eqs. (5)-(6) with $B_i = 0.4$ for the contact resistance estimated from experimental observations (Marshall et al., 1992; Chen et al., 1995). A recent research (Phelan et

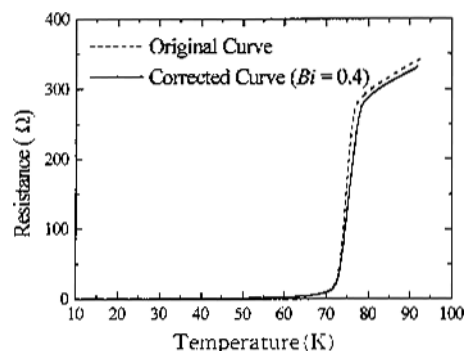


Fig. 3 Electrical resistances of the HTSC thin-film with respect to temperatures.

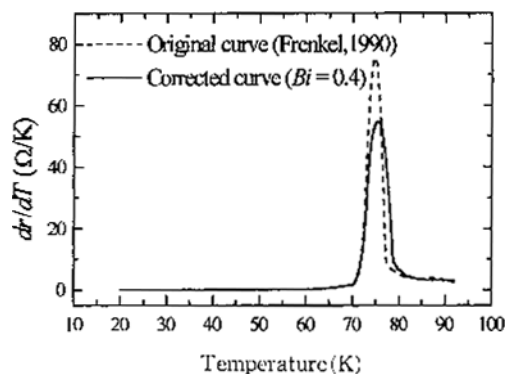


Fig. 4 Slopes of resistance-temperature curves of the HTSC thin-film.

al., 1994) reported that the contact resistance, R_b , ranged $1 \sim 5 \times 10^{-3} \text{ cm}^2 \text{ K/W}$. For temperatures below 70 K the resistance and Joule heating are so small that the corrected curve does not deviate from the experimental one. Since for temperatures above 70 K the electrical resistance increases very steeply and has a significantly large value, the film temperatures become greater than the substrate temperatures due to the corresponding Joule heating in the film, which results in the right-shift of r - T curve as shown in Fig. 3 from the experimental curve.

In Fig. 4, the slopes of r - T curves are plotted from the original experimental and corrected curves. This slope is very important to estimate the voltage response of the film, since the voltage response can be approximated as

$$\Delta V = I \frac{dr}{dT} \Delta T \quad (17)$$

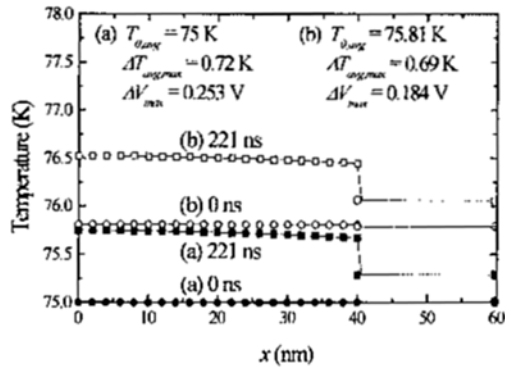


Fig. 5 Comparison between temperature profiles in the film and partially into the substrate for (a) initial uniform temperature distribution and (b) initial nonuniform temperature distribution ($T_0 = 75$ K, ILM, $Bi = 0.4$, $t_p = 200$ ns).

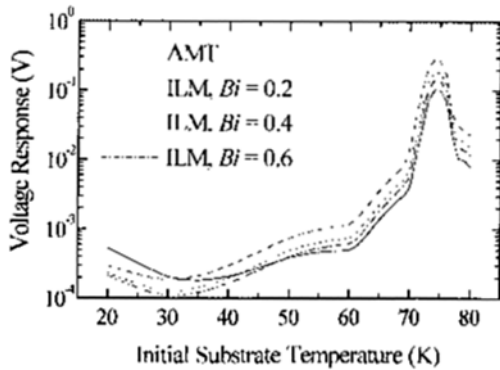


Fig. 6 Maximum voltage responses for several thermal contact resistances ($t_p = 200$ ns, $I = 5$ mA).

where ΔT is the average temperature change in the film. The comparison of the slopes shows that the voltage responses based on the corrected data can be much lower than the ones based on the original data at temperatures in the transition region and the former can be significantly greater than the latter at temperatures after the transition state.

Figure 5 shows initial and maximum temperature profiles in the film and partially into the substrate based on the initial uniform and nonuniform temperature distribution models. Without bias current, film and substrate temperatures are maintained at 75 K. The incident radia-

tion is a pulse of $t_p = 200$ ns described by Eq. (11), and Bi is 0.4 in the ILM.

Curves (a) are the results obtained from the initial condition of uniform temperature distribution, using Eq. (4). Initial film temperature, $T_{0,avg}$, at $t = 0$ ns is the same as the initial substrate temperature, 75 K, since there assumes no Joule heating even with the bias current. The predicted maximum average temperature of film, $T_{avg,max}$, is 75.72 K and theoretical maximum voltage response, ΔV_{max} , is 0.253 V. Curves (b) are obtained from the initial nonuniform temperature distribution which is the solution of Eqs. (5) – (6) and is depicted by the open circles. Due to the Joule heating the averaged initial film temperature, $T_{0,avg}$, is slightly increased even before the irradiation and is calculated as 75.81 K. The theoretical maximum film temperature, $T_{avg,max}$, reaches 76.5 K after the pulse irradiation and the corresponding ΔV_{max} is estimated as 0.184 V. As expected in Fig. 4, difference of the voltage responses from the two models is significant and the error of the uniform initial temperature model is about 37.5%.

In Fig. 6 maximum voltage responses, ΔV_{max} , as functions of initial substrate temperatures are compared to investigate the effects of thermal contact resistances. Thermal contact resistance is predicted by the AMT and the ILM for the range of Bi from 0.2 to 0.6. At temperatures below 32 K, Bi from the AMT is less than 0.2 and ΔV_{max} is greater than those from Bi in the ILM. In this temperature range, the AMT is known to yield the accurate prediction for the thermal contact resistance while the ILM overpredicts more or less. At temperatures between 32 K to 49 K, the AMT gives Bi of values between 0.2 and 0.6. Since Bi from the AMT becomes greater than 0.6 at temperatures above 49 K, ΔV_{max} predicted from the AMT is smaller than those from the ILM.

In Fig. 7 it is clearly described that the interfacial boundary resistance can be critical to the transient responses in the bolometers such as ΔV_{max} and the time lag between the peaks of the incident pulse and the film temperatures. Therefore, accurate information about thermal contact

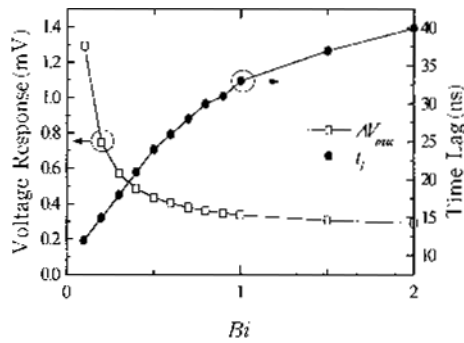


Fig. 7 Maximum voltage responses and time lags for various thermal contact resistances at 50 K (ILM, $t_p=200$ ns, $I=5$ mA).

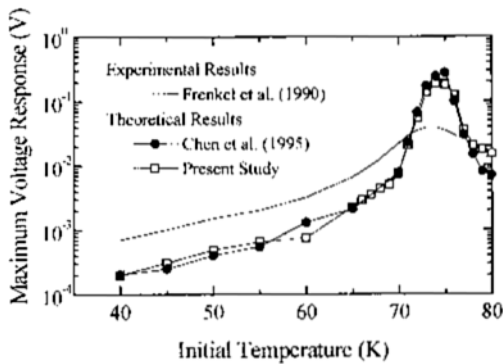


Fig. 8 Comparison of the calculated long-pulse maximum voltage responses with experimental data ($t_p=200$ ns, $I=5$ mA).

resistance should be in hand for the accurate prediction of the characteristics of the high- T_c superconducting bolometer.

A plot of maximum voltage responses, ΔV_{max} , versus initial temperatures, T_0 , for $I=5$ mA is given in Fig. 8. Predicted voltage responses are compared with the experimental observations from Frenkel et al. (1990) and previous theoretical predictions by Chen et al. (1995). For temperatures below the transition region, predicted voltage responses are smaller than the experimental ones and the differences are thought to be due to the nonbolometric responses.

For temperatures in the transition state, predicted voltage rises become significantly larger than those of experimental work, even though predictions of this study is more realistic than the

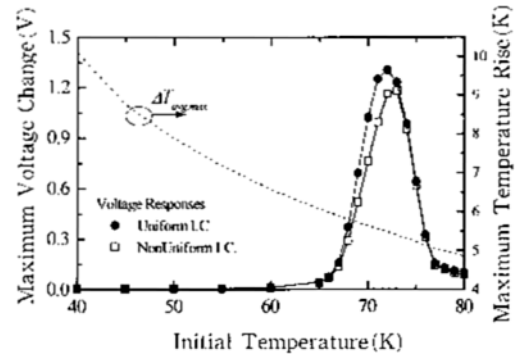


Fig. 9 Calculated maximum voltage responses and maximum change of average film temperatures for the shorter pulse ($t_p=150$ ps, $I=5$ mA, ILM, $Bi=0.4$).

previous one (Chen et al., 1995). Causes for this deviation between the theoretical and the experimental responses seem to be neglect of heat loss from the front surface ($x=0$), experimental errors in the measurement of substrate temperatures, inaccuracies involved in refractive indices and thermophysical properties, uncertainties in thermal contact resistance models, etc. These ambiguities demand more intensive research in this area.

A plot of maximum change in voltage and film temperature for a shorter optical pulse modeled in Eq. (12), as a function of initial substrate temperature, T_0 , is given in Fig. 9. Maximum rises of averaged film temperatures decrease monotonously with the initial substrate temperature due to the increase of heat capacity and thermal conductivity of the film and due to the accompanied decrease of thermal contact resistance. Differences between ΔV_{max} 's from the two initial condition models are slightly smaller than those expected from Fig. 4, since this short pulse is so intense that the film temperature increase is much larger than that for the longer pulse in Eq. (11), and that the state of the HTSC film changes from the superconducting to normal state where the slope of the $\gamma-T$ curve is relatively small.

Figure 10 compares one of other evaluation parameters for the transient decrease in voltage after passing the peak point, which is the fall time. Fall time, t_f , is defined as the time elapsed

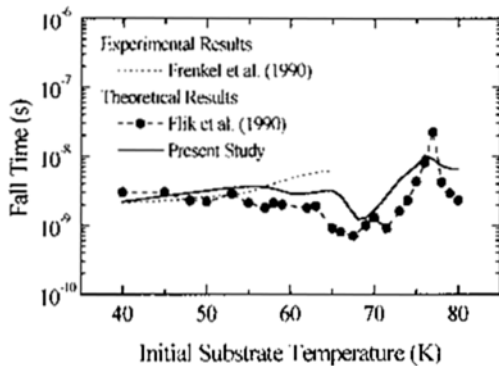


Fig. 10 Comparison between measured and calculated fall times for the shorter pulse ($t_p=150$ ps, $I=5$ mA).

between 90 and 10 % of the maximum voltage response. As apparent from in this figure, the experimental data and the numerical predictions do not agree exactly but show the same trend at temperatures below 55 K. The discrepancy at temperatures above 55 K becomes significant and might be attributable to uncertainties in the thermal mass of the film and thermal contact resistances, which require accurate measurements of those properties.

4. Concluding Remarks

A theoretical study is conducted to understand the fundamental physics of the HTSC thin-film bolometer exposed to an optical pulse with use of a one-dimensional radiation/conduction heat transfer model. The current model includes rigorous prediction of radiation absorption based on the electromagnetic theory for thin film, thermal contact resistance using the AMT and ILM, and nonuniform initial condition for the film/substrate temperature due to Joule heating before the radiation exposure.

Justification of the Fourier conduction model for this short pulse irradiation and thin film geometry is made using a simple kinetic theory.

Using the steady-state temperature solution the experimental resistance-temperature ($r-T$) curve, which is read with reference to the temperature of the substrate backside, has been corrected to be based on the film average temperature.

Since the voltage jump is proportional to the slope of the $r-T$ curve, the error involved in the estimation of the jump is recognized to be serious near the transition temperature, where the slope is very steep.

Though the voltage jump using the nonuniform initial condition approach the experimental jump nearer than the previous results based on uniform initial condition, still there is a big difference between the theoretical and experimental results.

Such a big difference seems to be caused by uncertainties and inaccuracies involved in thermal contact resistance models, film refractive indices, and specific heats of the film, which remain for future investigations.

Acknowledgements

This study is supported by Korean Ministry of Education through Research Fund No. ME96-A-17. Authors gratefully appreciate the support.

References

- Brasunas, J. C., Moseley, S. H., Lakew, B., Ono, R. H., McDonald, D. G., Beall, J. A., and Sauvageau, J. E., 1989, "Construction and Performance of a High-Temperature-Superconductor Composite Bolometer," *Journal of Applied Physics*, Vol. 66, pp. 4551~4554.
- Carr, G. L., Quijada, M., Tanner, D. B., Hirschmugl, C. J., Williams, G. P., Etemad, S., Dutta, B., DeRosa, F., Inam, A., Venkatesan, T., and Xi, X., 1990, "Fast Bolometric Response by High T_c Detectors Measured with Subnanosecond Synchrotron Radiation," *Applied Physics Letters*, Vol. 57, pp. 2725~2727.
- Chen, R. C., Wu, J. P., and Chu, H. S., 1995, "Bolometric Response of High- T_c Superconducting Detectors to Optical Pulses and Continuous Waves," *ASME Journal of Heat Transfer*, Vol. 117, pp. 366~372.
- Ferreira, J. M., Lee, B. W., Dalichaouch, Y., Torikachvili, M. S., Yang, K. N., and Maple, M. B., 1988, "Low-Temperature Specific Heat of the High- T_c Superconductors $\text{La}_{1.3}\text{Sr}_{0.2}\text{CuO}_{4-\delta}$ and $\text{RBa}_2\text{Cu}_3\text{O}_{7-\delta}$ ($R=\text{Y, Eu, Ho, Tm, and Yb}$),"

Physical Review B, Vol. 37, pp. 1580~1586.

Flik, M. I., Phelan, P. E., and Tien, C. L., 1990, "Thermal Model for the Bolometric Response of High- T_c Superconducting Films to Optical Pulses," *Cryogenics*, Vol. 30, pp. 1118~1128.

Frenkel, A., Saifi, M. A., Venkatesan, T., England, P., Wu, X. D., and Inam, A., 1990, "Optical Response of Nongranular High- T_c $Y_1Ba_2Cu_3O_{7-x}$ Superconducting Thin Films," *Journal of Applied Physics*, Vol. 67, pp. 3054~3068.

Fushinobu, K., Phelan, P. E., Hijikata, K., Nagasaki, T., and Flik, M. I., 1994, "Thermal Analysis of the Performance of a High- T_c Superconducting Microbolometer," *ASME Journal of Heat Transfer*, Vol. 116, pp. 275~278.

Hagen, S. J., Wang, Z. Z., and Ong, N. P., 1989, "Anisotropy of the Thermal Conductivity of $YBa_2Cu_3O_{7-x}$," *Physical Review B*, Vol. 40, pp. 9389~9392.

Kittel, C., 1986, *Introduction to Solid State Physics*, Wiley, New York.

Koo, J. M., 1996, "Thermal Analysis on the Voltage Response of High- T_c Superconducting Bolometers to Incident Radiation," Master Thesis, Hongik University.

Kumar, S. and Joshi, A., 1990, "Thermal Assessment of a Transition-Edge High- T_c Superconductor Infrared Detector," *Proc. AIAA/ASME Thermophysics and Heat Transfer Conference*, Seattle, WA.

Little, W. A., 1959, "The Transport of Heat between Dissimilar Solids at Low Temperatures," *Canadian Journal of Physics*, Vol. 37, pp. 334~339.

Marshall, C. D., Fishman, I. M., Dorfman, R. C., Eom, C. B., and Fayer, M. D., 1992, "Thermal Diffusion, Interfacial Thermal Barrier, and Ultrasonic Propagation in $YBa_2Cu_3O_{7-x}$ Thin Films: Surface-Selective Transient-Grating Experiments," *Physical Review B*, Vol. 45, No. 17, pp. 10009~10021.

Phelan, P. E., Song, Y., Nakabeppu, O., Ito, K., Hijikata, K., Ohmori, T., and Torikoshi, K., 1994, "Film/Substrate Thermal Boundary Resistance for an Er-Ba-Cu-O High- T_c Thin Film,"

ASME Journal of Heat Transfer, Vol. 116, pp. 1038~1041.

Richards, P. L., Clarke, J., Leoni, R., Lerch, Ph., Verghese, S., Beasley, M. R., Geballe, T. H., Hammond, R. H., Rosenthal, P., and Spielman, S. R., 1989, "Feasibility of the High- T_c Superconducting Bolometer," *Applied Physics Letters*, Vol. 54, pp. 283~285.

Slack, G. A., 1962, "Thermal Conductivity of MgO , Al_2O_3 , $MgAl_2O_4$, and Fe_3O_4 Crystals from 3 to 300 K," *Physical Review*, Vol. 126, pp. 427~434.

Streiffer, S. K., Lairson, B. M., Eom, C. B., Clemens, B. M., Bravman, J. C., and Geballe, T. H., 1991, "Microstructure of Ultrathin Films of $YBa_2Cu_3O_{7-\delta}$ on MgO ," *Physical Review B*, Vol. 43, No. 16, pp. 13007~13018.

Swartz, E. T. and Pohl, R. O., 1989, "Thermal Boundary Resistance," *Review of Modern Physics*, Vol. 61, pp. 605~668.

Touloukian, Y. S. and Buyco, E. H., 1970, *Thermophysical Properties of Matter*, Vol. 5, IFI/Plenum, New York, p. 140.

Tuntomo, A., Tien, C. L., and Park, S. H., 1991, "Internal Distribution of Radiant Absorption in a Spherical Particle," *ASME Journal of Heat Transfer*, Vol. 113, pp. 407~412.

van Miltenburg, J. C., Schuijff, A., Kadowaki, K., van Sprang, M., Koster, J. Q. A., Huang, Y. K., Menovsky, A. A., and Barten, H., 1987, "Specific Heat Measurements of High- T_c Superconductor $YBa_2Cu_3O_7$ Between 78 K and 260 K," *Physica*, Vol. 146B, pp. 319~323.

Zeldov, E., Amer, N. M., Koren, G., and Gupta, A., 1989, "Nonbolometric Optical Response of $YBa_2Cu_3O_{7-\delta}$ Epitaxial Films," *Physical Review B*, Vol. 39, No. 13, pp. 9712~9714.

Zorin, M., Lindgren, M., Danerud, M., Karasik, B., Winkler, D., Goltsman, G., and Gershenson, E., 1995, "Nonequilibrium and Bolometric Responses of $YBaCuO$ Thin Films to High-Frequency Modulated Laser Radiation," *Journal of Superconductivity*, Vol. 8, No. 1, pp. 11~15.